MORPHOLOGY AND MICROSTRUCTURE EVOLUTION OF COBALT FERRITE THIN FILMS PREPARED BY ONE-STEP MAGNETO-ELECTRODEPOSITION

LI[1,2] D., DALTIN[2] A.-L., WANG[1] Q., CHOPART[2] J.-P., HE[1] J.
[1] Key Laboratory of Electromagnetic Processing of Materials (Ministry of Education), Northeastern University, Shenyang, 110004, China
[2] LISM, Université de Reims Champagne-Ardenne, B.P. 1039, 51687 Reims Cedex 2, France
314 Box, Northeastern University, No.3-11 Wenhua Road, Shenyang, 110004, P.R.China
Tel:+86-24-83681726, Fax:+86-24-83681758, E-mail address:
wangq@mail.neu.edu.cn, al.daltin@univ-reims.fr

Abstract: In this paper, we report a one-step pulse-electrodeposition method assisted by a magnetic filed for preparing $Co_xFe_{3-x}O_4$ films on a Ti substrate. Grain shape, grain size, Co:Fe ratio, and microstructure in the $Co_xFe_{3-x}O_4$ films were modified dramatically by controlling the deposition potential during the pulse-electrodeposition process. The dependence of the grain shape and grain size on the deposition potential is due to the change of microstructure and Co:Fe ratio in the films with the potential induced by the MHD effects.

Keywords: *Cobalt ferrite; Thin Film; Microstructure; Pulse-electrodeposition; Magnetic fields*

1. Introduction

Due to their excellent electrochemical performance, higher magnetic anisotropy and moderate saturation magnetization, iron-cobalt oxides with spinel structures have attracted considerable interests as promising candidates for modern innovative applications such as gas sensors[1], catalysts for various reactions[2], anodes for lithium ion batteries[3], magneto-optic recording media[4]. Up to now, a variety of methods of synthesizing $Co_xFe_{3-x}O_4$ thin films have been developed include sputtering, physical vapor deposition, chemical vapor deposition, pulsed laser deposition and electrochemical deposition [5-8]. Most of these techniques involve a two-step process, the CoFe alloy precursors first formation, and then followed by oxidation at high temperature [9]. However, the high temperature annealing can cause unwanted reactions between the substrate and the deposited film, which affect the grain size, morphology, chemical stability and the magnetic property [10-11]. It is widely accepted that the practical application of $Co_xFe_{3-x}O_4$ thin films will depend on the capability of precise controlling the composition, particle size and structure during the preparation process. Magneto-electrodeposition could be an alternative method to obtain $Co_xFe_{3-x}O_4$ thin films by single-step at low temperature, with precise controlling the ratio of Co:Fe, morphology, and microstructure, furthermore to tailor the chemical and physical properties of the films. Recently, magnetic fields are widely used to control the mass transfer processes in electrochemical cells[12], since under a magnetic fields a Lorenz force arises, and the magnetohydrodynamics (MHD) convection governs the hydrodynamic boundary layers. Krause et al. [13] found that electrodeposition under a 1T magnetic field, Co deposit shape changed into double sized hexagonal crystallites. The previous study of us [14] also shown that magnetic fields induced drastic morphological variations in the electrodeposited CoNi films from short-clavated grain shape to silk-like nanowires, and the applied magnetic fields led to an increase of the Co:Ni ratio in the deposits. In addition,because of the higher instantaneous current density in comparison to direct current plating, pulse electrodeposition has been found to be an effective means of perturbing the adsorption/desorption processes and hence offers an opportunity of controlling the microstructure of the electrodeposits. This work presents one-step pulse-electrodeposition of Cobalt-Ferrite thin film on the Ti substrate under a 1T magnetic fields. The aim of this work is to study the evolution of composition, surface morphology, and microstructure of cobalt ferrite thin films under the condition of magneto-pulse-electrodeposition.

2. Experimental

All electrodeposition experiments were performed in a conventional three-electrode cell without agitation. Polished titanium of 1cm diameter was used as the working electrode, the counter electrode was a quadrate Pt plate of $1 \times 1cm$, and Ag/AgCl/KNO_3(sat.) was used as a reference electrode. The electrolyte composed of 100mM Co^{2+} 50mM Fe^{3+} , 150mM triethanolamine (TEA), and 2M NaOH. Pulse-electrodeposition using a potentiostat-galvanostat VersaSTAT 4 was performed at 80 . The electrochemical cell was plunged into the gap of Drusch EAM 20G electromagnet that delivers a uniform horizontal magnetic field up to 1T parallel to the electrode surface. To deposit good quality films, various parameters such as deposition potential, magnetic flux density, deposition time and duty cycle etc., were optimized as shown in Table.1.

Table 1. Processing conditions of electrodeposition of the cobalt ferrite films

Pulse-potential $V1_{Ag/AgCl}$	Deposition time, t1	Pulse-potential $V2_{Ag/AgCl}$	Deposition time, t2	Cycles	Magnetic field
-1.17V~-1.19V	1s	-0.95V	4s	300	1T

The surface morphology and chemical composition of the deposited films were investigated by scanning electronic microscopy (SEM) appended with an energy-dispersive X-ray spectroscope (EDX, SUPRA 35) at three different positions on the films. The topography were investigated with atomic force microscopy (AFM). For the characterization of the microstructure of the films, X-Ray Diffraction (XRD, Bruker D8 Advance) measurements were performed using standard θ-2θ geometry with Cu $K\alpha$ radiation.

3. Results and discussion

Since in case of without magnetic field, the electrodeposited films obtained under the experimental condition in this work were not adherent and covered the substrates bad, all the electrodeposition were optimized by performing in a 1T magnetic field. Typical SEM and AFM morphologies of cobalt ferrite films pulse-electrodeposited with potential ranged from -1.17V to -1.19V$_{Ag/AgCl}$ are shown in Fig. 1.

The figure demonstrates drastic morphological variations with the pulse-potential during the electrodeposition process. The spherical grain linked together to form a coralliform morphology as shown in Fig.1(a). While in case of the potential up to -1.18V$_{Ag/AgCl}$, the top of the branches in coral seemed to split into many irregular small grains. With the increase of the applied potential to -1.19V$_{Ag/AgCl}$, the grains of this coralliform deposit is very similar to the structure of sea anemones, that is, every spherical grain consisted of many crystal whiskers in it. Since the difference in surface analysis between AFM (3D overview in perpendicular to the surface) and SEM (2D morphological structure in parallel to the surface), the AFM image could not answer the morphology evolution of the films, but shown the films are composed of fairly large number of round nanometer sized grains. The average values of lateral feature size, which can be used to characterize the grain size, were calculated according to AFM images in the following section.

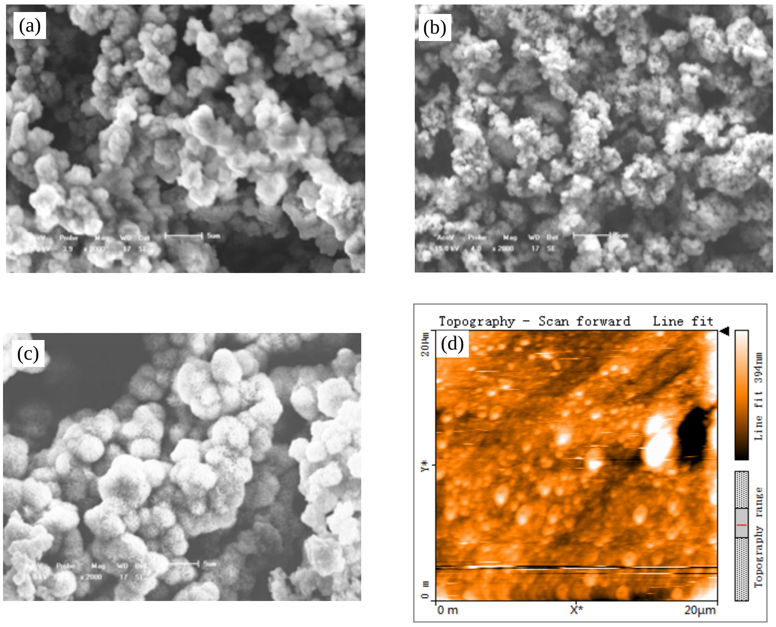

Figure 1: SEM images of $Co_xFe_{3-x}O_4$ thin films deposited at (a) -1.17V $_{Ag/AgCl}$; (b) -1.18V$_{Ag/AgCl}$; (c) -1.19V$_{Ag/AgCl}$ potentials assisted by 1T magnetic field; and the typical AFM image at (d) -1.18V$_{Ag/AgCl}$.

Corresponding to the evolution of the morphology, we use the EDX to measure the change of composition in the deposited films with different pulse-potentials. The results in Tab. 2 shown that the Co:Fe ratio depended on the deposition potential. The Co concentrations in the films were lower at less negative potentials and higher at more negative potentials. With the deposition potential went to more negative values, more Co^{2+} were reduced at the electrode surface, resulting in a increase of the Co:Fe ratio in the film. These phenomena may be attributed the MHD effect in a magnetic field, which yields significant convection, and in turn increases the current efficiency. However due to the different kinetic reaction rate between Fe^{3+} and Co^{2+} substitution, the deviation between the Co concentration and Fe concentration at the electrode surface was larger when the growth rate of the film was faster at more negative potentials caused by the MHD effect[15]. The deviation resulted in the Co:Fe ratio in the $Co_xFe_{3-x}O_4$ thin films a non-linear variation with the deposition potential. In case of -1.18V$_{Ag/AgCl}$, the x value was 0.97, which indicates that the film obtained under this condition was composed of almost $CoFe_2O_4$. This can be verified in the X-ray diffraction pattern.

Table 2. The dependence of the composition of $Co_xFe_{3-x}O_4$ 0 x 1 films on the deposition potentials: the x value in $Co_xFe_{3-x}O_4$ was calculated based on the Co:Fe ratio in the films.

Pulse-potential	Co (at%)	Fe (at%)	O (at%)	x
-1.17V $_{Ag/AgCl}$	8.6	31.1	60.3	0.65
-1.18V $_{Ag/AgCl}$	14.2	29.9	55.9	0.97
-1.19V $_{Ag/AgCl}$	12.1	30.5	57.4	0.85

The X-ray scan of the $Co_xFe_{3-x}O_4$ films pulse-electrodeposited on titanium were shown in Fig.2. Despite of the high peaks (marked with black dots) for the substrate (Ti), the films exhibited the diffraction peaks corresponding to both the transition metal oxides (Fe_2O_3) and the spinel cobalt ferrite ($CoFe_2O_4$). At less negative potential, the film was mostly composed of

Fe_2O_3, while at more negative potentials, the films was mostly composed of $CoFe_2O_4$. Especially at -1.18$V_{Ag/AgCl}$, the said planes as (111),(220),(311),(400),(511) corresponded to the $CoFe_2O_4$. The peaks shown in Fig 2 agree well with the Co:Fe ratio measured by EDX. For example, the x value in $Co_xFe_{3-x}O_4$ films was near unit at -1.18$V_{Ag/AgCl,}$ which implied that by adjust the potential assisted by magnetic field, we could prepare spinel cobalt ferrite without other oxidations by one-step magneto-electrodeposition method.

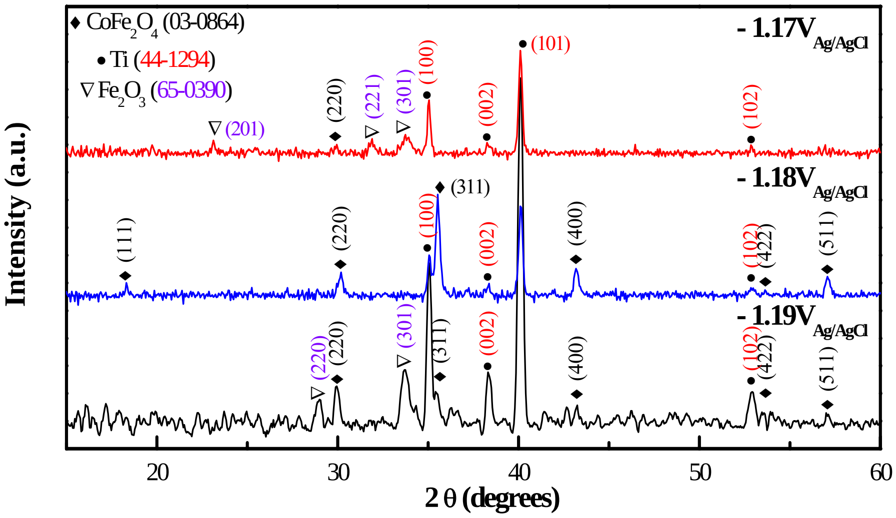

Figure 2: The X-ray diffraction pattern of cobalt ferrite films deposited at different potentials.

Table 3. Comparison of crystallites size of electrodeposited $Co_xFe_{3-x}O_4$ films obtained by calculations based on the Scherrer equation and AFM

Potential ($V_{Ag/AgCl}$)	Sherrer(nm)	AFM (nm)
-1.17	33	47±2
-1.18	25	38±2
-1.19	50	61±2

Since the morphology and microstructure of the films were dramatically depended on the potential during the electrodeposition, the grain size should also be affected by the MHD effect caused by the interaction between the pulse-current with the magnetic field. We have calculated the crystallites size by use of Scherrer's equation and AFM measurement (Table. 3). The particle size R_0 was estimated from AFM analysis by the following equation [16]: $R_0 = \left(\frac{A_0}{\pi N_0}\right)^{1/2}$, in which A_0 represents the AFM total image area and N_0 is the grain number. According to these two calculated methods the obtained films consisted different nuclei sizes due to the changing amplitude of pulse-potential. It should be mentioned that the calculated mean grain size by using Scherrer’s formula according to the X-ray diffraction share the same trend as that measured based on the AFM images. With the potential moving to more negative, the MHD effects [17] increase to bring more $Co^{2+}(Fe^{3+}$ to the surface of the electrode, which results in the fast nucleation and is responsible for the small grain size at -1.18 $V_{Ag/AgCl}$. However, in case of -1.19 $V_{Ag/AgCl}$, the Co (Fe) deposition becomes to be diminished, since the hydrogen-ion reduction dominates the total reduction process resulting in the decrease of the current efficiencies of Co (Fe). This may be a reason for the formation of bigger grain by growth at more higher pulse-potential.

From the morphological viewpoint, the properties of the electro-deposited films depend not only on the chemical position, but also strongly on the morphology, grain size ,and microstructure [18-19]. Therefore, the in-situ application of magnetic field during the pulse-electrodeposition is exceptionally well suited for tailoring the properties of cobalt ferrite, by non-contact controlling Co:Fe ratio, grain shape, grain size and phase composition. The present work paves the way for optimized electroplated cobalt ferrite thin films by adjusting the potential during one-step magneto-electrodeposition.

4. Conclusions

The influence of the interaction between the pulse-potential and a magnetic field with a flux density up to 1T on the morphology and microstructure of electrodeposited $Co_xFe_{3-x}O_4$ film has been investigated. The SEM figures demonstrated that MHD effects induced drastic morphological variations from coral-like to sea-anemone-like. More negative potential led to an increase of the Co:Fe atomic ratio in the deposits. The XRD pattern further verified that at $-1.18V_{Ag/AgCl}$ we could obtain $CoFe_2O_4$ film with ultra-fine grains in it by one-step magneto-electrodeposition. The non-monotonic dependence of morphology, composition, and microstructure on pulse-potential may be attributed to the overlap effects of MHD on the current efficiency and on the hydrogen-ion reduction during the deposition process.

Acknowledgments. This work was financially supported by the National Natural Science Foundation of China (Grant No. 51101032), the Fundamental Research Funds for the Central Universities (Grant No. N130402002), Agence Nationale de la Recherche France (Programme COMAGNET, Grant No. 2010-INTB-903-01).

References

[1] Said A. A; El Salaam K, M. A.; Hassan E. A.; Elawad A. M.; Elwahab M. M. M. A.: J. Phys. IV, 7 (1997) 687-688.
[2] Chaudhari G. N.; Pawar M. J.; Optoelectron J.: Adv. Mater., 10 (2008) 2574-2577.
[3] Sharma Y.; Sharma N.; Rao, G. V. S.; Chowdari B. V. R.: Solid State Ionics., 179 (2008) 587-597.
[4] Giri A. K.; Kirkpatrick E. M.; Moongkhamklang P.; Majetich S. A.; Harris V. G.: Appl. Phys. Lett. 80 (2002) 2341-2343.
[5] Zhou J. P.; He H. C.; Nan C. W.: Appl. Surf. Sci., 253 (2007) 7456-7460.
[6] Sartale S. D.; Ganesan V.; Lokhande C. D.: Phys. Status Solidi A., 202 (2005) 85-94.
[7] Araujo C.; Almeida B. G.; Aguiar M.; Mendes J. A.: Vacuum, 82 (2008) 1437-1440.
[8] Lokhande C. D.; Kulkarni S. S.; Mane R. S.; Nandi K. C.; Han S. H.: Curr. Appl. Phys., 8 (2008) 612-615.
[9] Hua Z. H.; Chen R. S.; Li C. L.; Yang S. G.; Lu M.; Gu B. X.; Du Y. W.: J. Alloy. Compd., 427 (2007) 199-203.
[10] Castaldi L.; Giannakopoulos K.; Travlos A.; Niarchos D.: Appl. Phys. Lett. 85 (2004) 2854-2856.
[11] Li D. G.; Levesque A.; Wang Q.; Franczak A.; Wu C.; Chopart J. P.; He J. C.: CMC-Comput. Mater. Con., 670 (2012) 1-12.
[12] Koza J. A.; Karnbach F.; Uhlemann M.; McCord J.; Mickel C.; Gebert A.; Baunack S.; Schultz L.: Electrochim. Acta., 55 (2010) 819-831
[13] Krause A.; Hamann C.; Uhlemann M.; Gebert A.; Schultz L.: J. Magn. Magn. Mater. 290-291 (2005) 261-264.
[14] Li D. G.; Levesque A.; Franczak A.; Wang Q.; He J. C.; Chopart J. P.: Talanta 110 (2013) 66-70.
[15] He Z.; Koza J. A.; Mu G. J.; Miller A. S.; Bohannan E. W.; Switzer J. A.: Chem. Mater., 25 (2013) 223-232.
[16] Raoufi D.: App. Surf. Sci., 255 (2009) 3682-3686.
[17] Koza J. A.; Uhlemann M.; Gebert A.; Schultz L.: Electrochim. Acta., 53 (2008) 5344-5353.
[18] Armyanov S.: Electrochim. Acta. 45 (2000) 3323-3335.
[19] Ergeneman O.; Sivaraman K.M.; Pané S.; Pellicer E.; Teleki A.; Hirt A.M.; Baró M.D.; Nelson B.J.: Electrochim. Acta 56 (2011) 1399-1408